

Modeling and Analysis of the Interactions of Coherent Structures with a Spray Flame in a Swirl Burner

L. Guedot, G. Lartigue and V. Moureau

Abstract With the constant increase in super-computing power, Large-Eddy Simulation (LES) has become an important tool for the modeling and the understanding of flame dynamics in complex burners. A fine description of the reaction layers in such devices requires fine meshes and the resolution of a broad range of turbulent scales. Unfortunately, extracting the large-scale features is not trivial. To this aim, implicit high-order filters that are based on simple low-order finite-volume operators have been proposed. These filters are applied in the LES of the MERCATO burner in order to study the complex interactions of the Precessing-Vortex Core, a large vortex typical of swirl burners, and a spray flame. High-order filters conveniently enable the analysis of the flame anchoring and its dynamics in the wake of the PVC.

1 Background and Motivation

1.1 Main Features of Swirling Flows

Swirling jet flows are widely used in combustion devices for the stabilization of premixed or partially premixed flames. This stabilization is made possible by the vortex breakdown that occurs when the geometric swirl number, which measures the ratio of tangential over axial momentum flux, is sufficient. The swirl generates a pressure decrease near the axis that leads to the formation of an axial recirculation zone. In such flows, incoming gases are slowed down by the recirculation zone that acts as an aerodynamic blockage, and the reaction zone is fed with recirculating hot gases

L. Guedot · G. Lartigue · V. Moureau (✉)
CORIA - CNRS UMR 6614, Normandie Université, Université et INSA de Rouen,
Saint Etienne du Rouvray, France
e-mail: vincent.moureau@coria.fr

ensuring the stability of the flame [13, 17]. In some conditions, the vortex breakdown may also lead to the formation of coherent structures such as the Precessing Vortex Core (PVC) [13, 23], which consists of single or multiple helical vortices.

The PVC plays an important role in the dynamics of the flow, and this instability has been widely studied, as reveals the extensive literature addressing this issue. Based on modal analysis of experimental data, some authors showed that the PVC may be responsible for local extinction of the flame or auto-ignition, and strongly interacts with the flow [1, 22]. The PVC may also wrinkle the premixed flame front creating isolated flame pockets [23]. The wrinkling and stretching of the flame surface leads to periodic fluctuations of the heat release rate, that might affect the acoustic behavior of the chamber. Some recent studies [21] showed that the PVC can either amplify or damp acoustic instabilities, according to the respective position of the PVC and the flame, highlighting the complexity of the phenomenon. In the same perspective, Caux-Brisebois et al. developed an advanced post-processing method of experimental data to study the coupling between acoustic instabilities and the PVC, and predict the burner stability [2].

In the case of spray flames, the PVC also influences the distribution of fuel mass fraction as it leads to preferential segregation of fuel droplets [18, 20]. Some recent work [10] showed that the high level of turbulence due to the PVC close to the fuel injection helps the atomization process and the development of small droplets, improving the efficiency of the device. The influence of the PVC in two-phase reacting flows results in complex coupling mechanisms. The analysis of this large-scale feature is mandatory to improve the understanding of the dynamics of swirling flows.

Guedot et al. [7] recently proposed high-order implicit filters for the extraction of large scales in complex geometries. These filters were successfully applied to the identification of large vortices in the isothermal flow in a complex swirl burner. The aim of the present paper is to apply the same methodology to all the available data found in high-fidelity Large-Eddy Simulations in order to identify the dominant interactions in a semi-industrial spray burner.

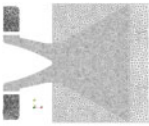
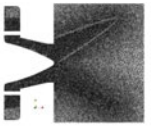
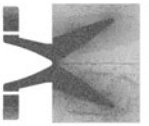
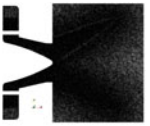
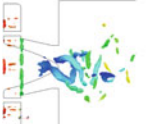
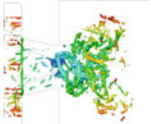
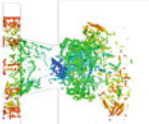
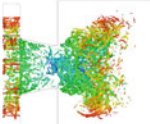
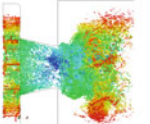
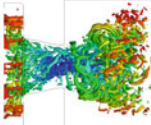
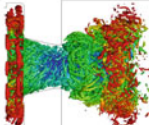
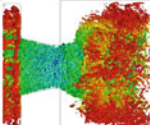
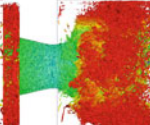
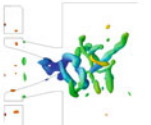
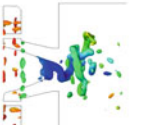
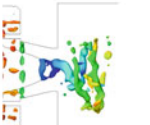
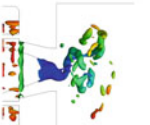
1.2 Extraction of Large-Scale Structures in High-Fidelity Simulations

Large-Eddy Simulation is a powerful tool for the analysis of coherent structures in turbulent flows. The steady increase in computational power leads to finer and finer mesh resolutions, which enables an accurate prediction of all flow features. As a result, large scale simulations with meshes up to several billion cells are currently performed on massively parallel machines using thousands of processors. The analysis of these billion-cell simulations is very challenging because it requires to handle a large amount of data, and traditional data processing tools have to be redesigned to post-process and analyze large scale simulation. In particular, the extraction of large scale structures becomes very challenging when dealing with highly refined

meshes. High-fidelity simulations provide solutions that contain a wide range of length-scales, ensuring a good description of the physics, but making it difficult to extract relevant information among the large amount of data it generates.

A convenient tool for the visualization of coherent vortices is the Q-criterion, which is the second invariant of the deformation tensor [9]. The Q-criterion is related to the Laplacian of the pressure field in incompressible flows [4]. For homogeneous isotropic turbulence, the scaling power of the Q-criterion with the wave number k is larger than unity [16]. The Q-criterion exhibits larger values for small vortices than for big vortices, because the smallest vortices have a greater velocity gradient. This issue is particularly annoying in well refined simulations that feature a large range of turbulent scales. In these simulations, the small vortices completely mask the large vortices when looking at Q-criterion iso-values as shown with the iso-surfaces of unfiltered Q-criterion in Table 1). This problem is illustrated here in the simulation of a semi-industrial swirl burner operated in the PRECCINSTA European project.

Table 1 Extraction of the PVC with unfiltered and filtered Q-criterion in the LES of the PRECCINSTA burner at various mesh resolutions from 3 million to 878 million tetrahedral elements. The vortices are colored by the axis distance

	3 M	14 M	41 M	110 M	878 M
Mesh					
Q-criterion	 $Q = 0.32 \times 10^8$	 $Q = 0.8 \times 10^8$	 $Q = 1.5 \times 10^8$	 $Q = 2 \times 10^8$	 $Q = 5 \times 10^8$
Q-criterion	 $Q = 0.32 \times 10^8$	 $Q = 0.32 \times 10^8$	 $Q = 0.32 \times 10^8$	 $Q = 0.32 \times 10^8$	 $Q = 0.32 \times 10^8$
Filtered Q-criterion	 $\bar{Q} = 0.32 \times 10^8$	 $\bar{Q} = 0.32 \times 10^8$	 $\bar{Q} = 0.32 \times 10^8$	 $\bar{Q} = 0.32 \times 10^8$	 $\bar{Q} = 0.32 \times 10^8$

The Q-criterion has already been used to visualize the PVC on coarse grids in this configuration [14, 19] but an issue appears for highly refined simulations. This issue is illustrated in Table 1. A Q-criterion iso-surface is used to visualize the PVC, on 5 meshes from 3 million to 878 million tetrahedral cells. The method performs well on the coarse grid but appears to be inefficient on refined grids. A low Q-criterion threshold must be chosen to capture the PVC since it is a large scale vortex compared to the smaller resolved scales. But since the Q-criterion of the smallest vortices is larger than the one of the large coherent structures, the PVC is masked by small-scale surrounding turbulence. When choosing a higher threshold, only the smaller vortices can be observed. The Q-criterion is a good candidate for vortices extraction but it is limited to the visualization of vortices of characteristic length-scale close the smallest scales resolved on the mesh.

To circumvent the Q-criterion scaling issue, it is mandatory to develop numerical techniques able to perform scale separation of the different coherent structures, such as spatial low-pass filters. This filtering operation is challenging as it requires to extract features from a large amount of data distributed across a large number of processors. This operation necessitates a good selectivity in order to leave the large scales unaffected while damping all the smallest scales. To this aim, high-order filters were implemented in the Large-Eddy Simulation (LES) solver YALES2 [15], and applied in an aeronautical swirl burner as depicted in Fig. 1 [7]. This figure shows that the PVC is successfully extracted from these highly refined simulations when filtering the Q-criterion at a high order.

2 Application to a Realistic Swirling Two-Phase Flow in Reactive Conditions

2.1 Operating Conditions

In this section, the MERCATO test-rig [11] is simulated in reactive operating conditions. First, the simulation is initiated with purely gaseous flow. Fresh gases are injected at the inlet at 293 K. Then particles are injected, and combustion is initiated with a heat source. Once steady state is reached, statistics are accumulated over 150 ms. Axial velocity measurements are available for the liquid and the gaseous phase in planar sections located at 10, 26, 56 and 116 mm of the injection plane. The operating conditions are summarized in Table 2. Under these conditions, the Reynolds number based on the diameter of the swirler exit and the bulk velocity is approximately $Re = 54\,000$ and the swirl number $Sw = 0.7$.

Table 2 Operating conditions

T_{air} (K)	T_{fuel} (K)	\dot{m}_{air} (g/s)	\dot{m}_{fuel} (g/s)	P (Pa)
293	300	35	2.25	101 300

2.2 Numerical Setup

A two-step chemical scheme was used to describe the kinetics of reaction [5]. To take into account the flame/turbulence interaction, the TFLES model was chosen [3, 12]. It artificially thickens the flame front according to a dynamic flame sensor based on a progress variable source term, which is the sum of the species mass fractions of CO, CO₂ and H₂O.

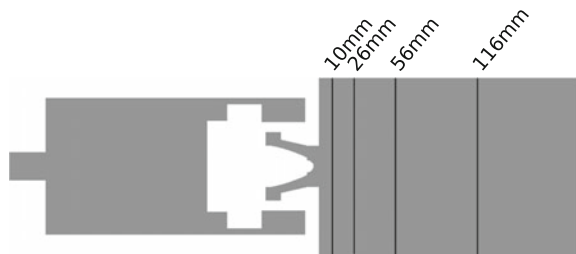
2.3 Mean Flow Statistics

Mean gaseous and liquid velocities extracted in the sections given by Fig. 1 are represented in Figs. 2 and 3 and compared to those obtained experimentally and with LES by [8]. The flow is characteristic of swirl burners with a large central recirculation. The global flow topology and the amplitude of the mean and RMS velocity profiles are well reproduced. The size of the central recirculation zone is over-estimated in the two first planes, but in good agreement with the simulations of Hannebique [8]. The profiles at 56 and 116 mm from the injection plane are in excellent agreement with the experiments.

2.4 Flame Anchoring Dynamics

The flow dynamics in the swirl burner is dominated by a periodic motion that appears close to the injection plane. Figure 4 shows temperature and mixture fraction fields in the mid-plane at successive times. The anchoring point in the central recirculation zone periodically oscillates from top to bottom in the mid-plane. The period of this fluctuation is approximately 0.9 ms, which is in good agreement with the PVC frequency, measured experimentally at 1050 Hz [11]. The flame anchoring is a key parameter for the stability of the combustor. To track the location of this point over several PVC periods, high-order filtering was used to extract the most backward axial position in the burnt gases within the injection area. The extraction algorithm,

Fig. 1 Axial position of the profiles in the burner



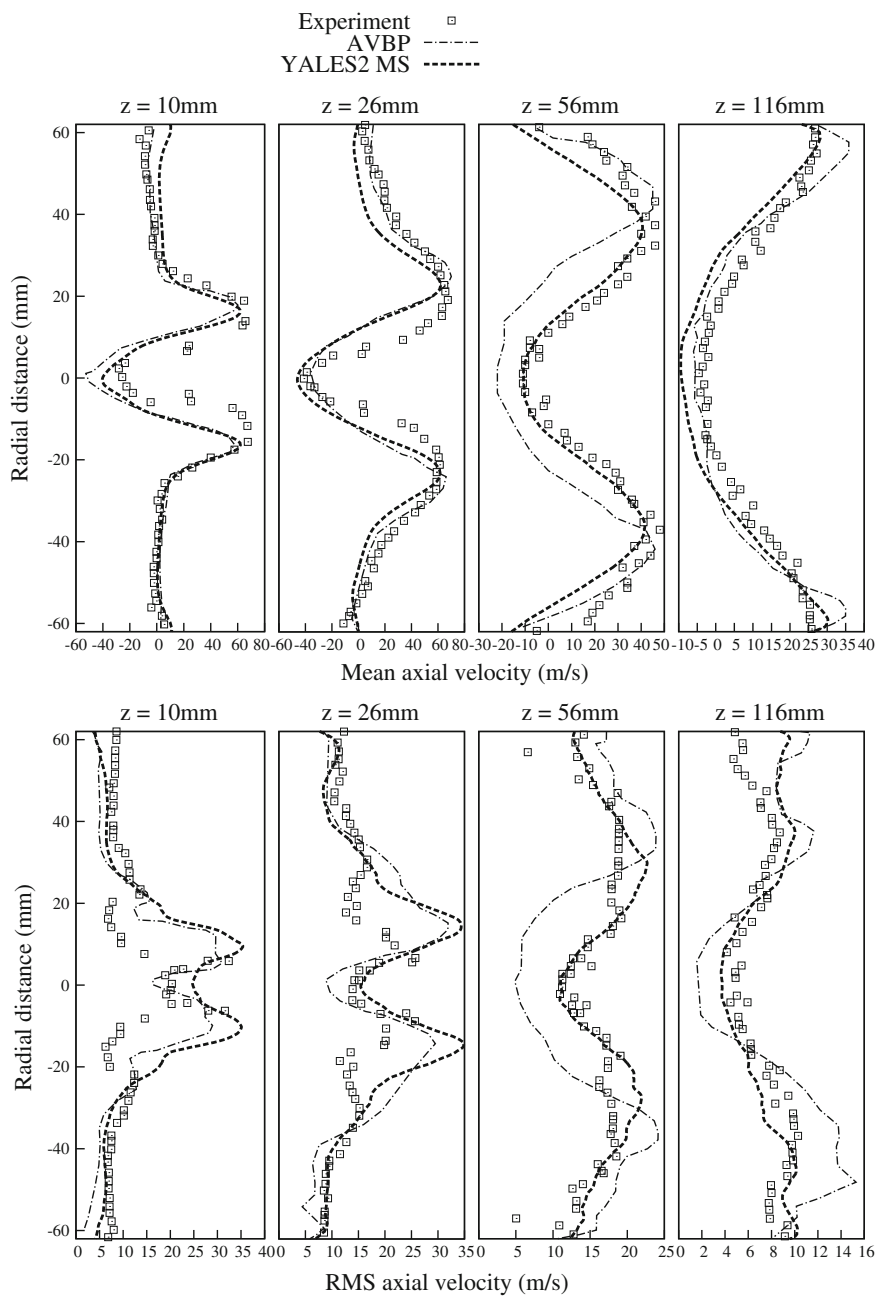


Fig. 2 Mean gaseous velocity profiles

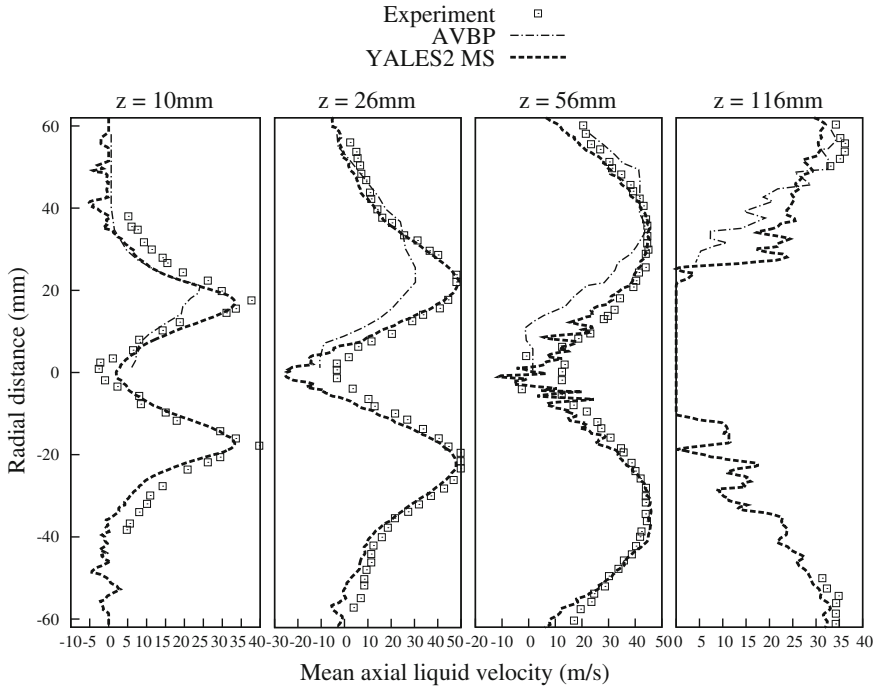


Fig. 3 Mean liquid velocity profiles

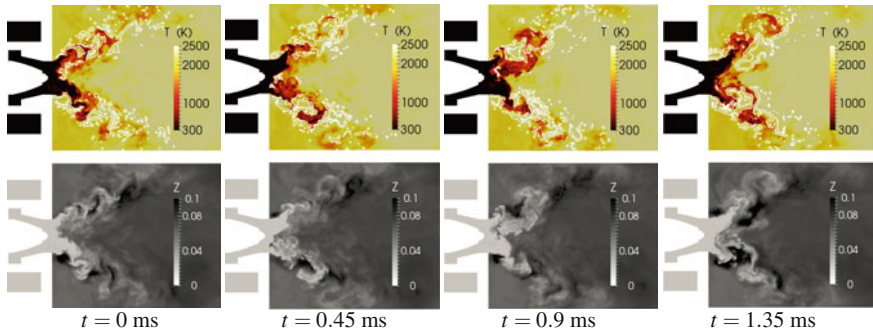


Fig. 4 Mixture fraction and temperature for four successive instants. The view is limited axially to $Z = 150$ mm. The central recirculation zone anchoring has a periodic motion inside the swirler

illustrated in Fig. 5 consists of filtering the temperature, and segmenting the image based on the $\bar{T} = 1100$ K iso-surface. The anchoring point is defined as the mesh point of the filtered iso-surface with the most backward axial coordinate. The research area is narrowed to a small volume from the injection plane to two exit diameters downstream, and within a radial distance smaller than the exit diameter.

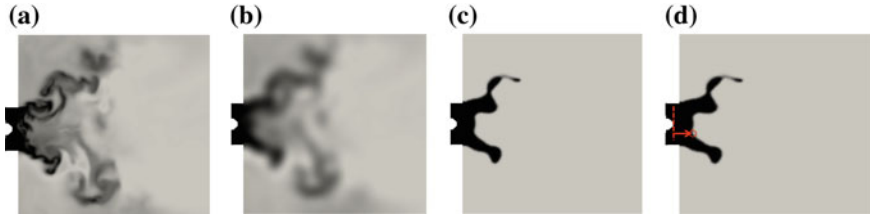


Fig. 5 **a** Temperature, **b** high-order filtered temperature, **c** segmentation based on the filtered temperature iso-surface $\bar{T} = 1100$ K, and **d** determination method of the anchoring point. The view is limited axially to $Z = 130$ mm

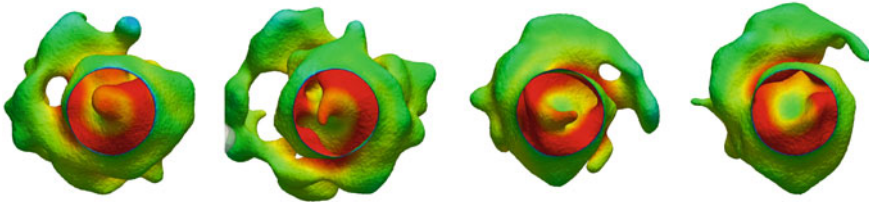


Fig. 6 Rotation of the anchoring point, visualized by iso-surfaces of filtered temperature. Snapshots are taken every 0.22 ms

The filtered flame surface is represented in Fig. 6, where its rotation is clearly visible. The rotation direction matches the one of the precessing movement of the PVC, and of the swirl motion in the burner. The flame surface however wraps around the central recirculation in the opposite rotation direction. It was verified (not shown here) that over more 10 PVC periods, the anchoring point follows an almost perfect circle. All the collected points are gathered around 6mm from the rotation axis, and at 10 mm from the combustor head, with small fluctuations in the axial direction.

2.5 *Spray-PVC-Flame Interactions*

In this section, the interactions of the PVC with the spray flame are analyzed more in details. The objective is to show that high-order filters enable to gain a deeper insight into the large-scale dynamics of the spray flame. This analysis complements the study of [6], who investigated the dynamics of swirling propane/air flames. They found that the flame stabilization point follows a helicoidal trajectory, which is phase-shifted with the PVC. The present study aims at extending this analysis to spray flames. High-order filters were used at order 8 and with a filter size of $\Delta = 12$ mm to filter all the available data such as Q-criterion, temperature, kerosene mass fraction, evaporation rate, reaction rate and velocity.

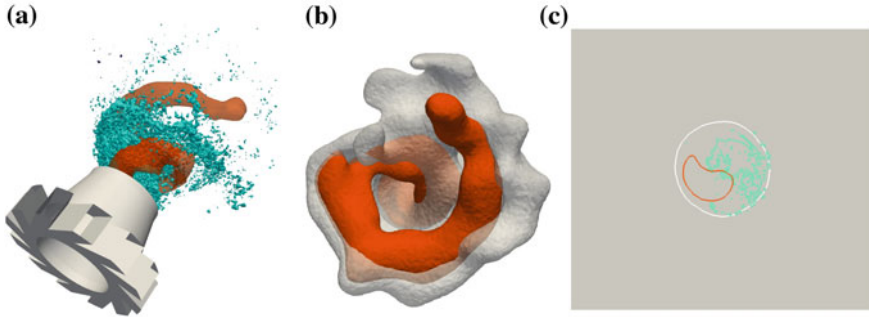
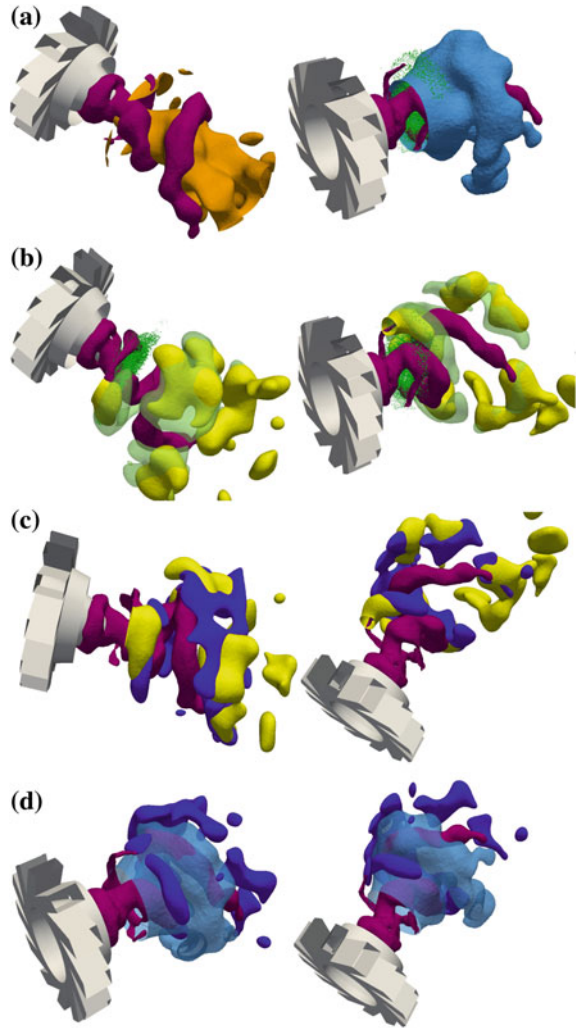


Fig. 7 Filtered temperature iso-surface to represent the flame (*white*), filtered Q-criterion iso-surface to show the PVC (*orange*), and spray droplets (*blue*) inside the burner (**a**), (**b**), and in a planar section at 6 mm of the combustor head (**c**)

Figure 7 shows iso-surfaces of filtered Q-criterion and temperature to materialize the PVC and the flame surface, respectively. The latter follows the helical shape of the PVC. This phenomenon is responsible for the periodic release of hot pockets convected to the outlet, and the periodic heat release observed experimentally in this type of burner. The Fig. 7a, c show that the presence of the PVC breaks the initial symmetry of the spray. At 6 mm from the injection plane, the spray is swept away by the PVC, and particles are concentrated in the azimuthal portion of the plane opposite to the PVC. This phenomenon, combined with the precessing movement of the PVC generates a precession of the spray that follows the PVC, and gives a helical shape to the spray droplets.

Iso-surfaces of all filtered variables are displayed in Fig. 8 in order to highlight the complex interactions between the PVC and the spray flame. As explained earlier, the spray is asymmetric and droplets are gathered away from the rotation axis of the swirler due to the PVC motion. Fuel droplets start evaporating as soon as they encounter hot burnt gases in the inner and outer recirculation zones. Because of the segregation of the fuel droplets due to the PVC, local rich pockets of gaseous fuel are generated when the droplets evaporate. The dynamics of these rich fuel pockets is the same as the one of the fuel droplets: the spatial distribution of the evaporated kerosene is helically shaped and follows the PVC with a phase shift. The fuel released in these rich pockets starts burning in a diffusion regime. This combustion regime was assessed by plotting the Takeno flame index (not shown here). The remaining fuel is then mixed by turbulence and burns in a premixed regime further downstream. Larger particles, with higher evaporation time-scales, disappear further away in the burnt gases, generating small isolated reaction zones.

Fig. 8 Iso-contours of filtered Q-criterion (*dark pink*), of filtered axial velocity (*orange*), of filtered temperature (*light blue*), of filtered kerosene mass fraction $\bar{Y}_{kero} = 0.01$ (*yellow*), filtered fuel evaporation rate $\bar{\omega}_{kero, evap}$ (*transparent green*), filtered enthalpy source term $\bar{\omega}_T$ (*dark blue*) and spray droplets (*green*) for the same snapshot in the vicinity of the injector



To ease the understanding of the complex PVC/spray flame interactions, a sketch based on the observation of all the filtered variables at several chosen instants is shown in Fig. 9. The sketch represents the interlacing of the important zones of the flow: the PVC, the fuel droplets, the evaporated fuel pockets and the heat release fronts. This figure again highlights the strong impact of the PVC on the dynamics of the flow.

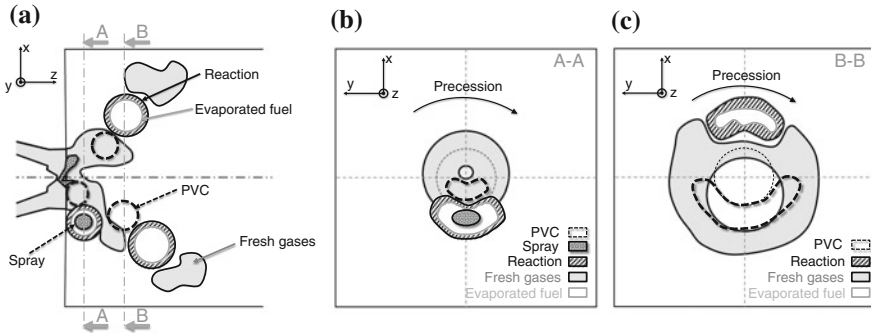


Fig. 9 Illustration of the PVC/spray flame interactions. **a** side view, **b** and **c** view of planes that are orthogonal to the burner axis

3 Conclusions

Simulations of the MERCATO burner were carried out in reactive flow conditions with liquid fuel injection. These simulations were validated against experimental and numerical data obtained by another group. The objective of the paper was to demonstrate the potential of implicit high-order filters to extract the large-scale dynamics of the flow even for complex burners. In particular, the flow in the MERCATO burner exhibits a strong Precessing Vortex Core, which imposes its dynamics to the spray and the flame. This leads to periodic fluctuations of the flame anchoring and of the heat release in the burner at the PVC frequency.

In this paper, a single set of operating conditions was investigated. The analysis, which was carried out may be different if the droplet diameter distribution changes. Indeed, the segregation effect of the PVC on the fuel droplets is directly related to the diameter distribution. Changing the PVC related Stokes number may reduce the segregation of the fuel droplets and reduce the interactions. Studying other sets of operating conditions would also be interesting to know if the PVC has a positive or negative impact on the global performances of the burner: compactness of the flame, lean blow-out limits, pollutant emissions.

Acknowledgements Computational time was provided by GENCI (Grand Equipement National de Calcul Intensif) under the allocation x20152b6880, and all simulations were performed on the HPC ressources of IDRIS, TGCC and CINES.

References

1. Boxx I, Stöhr M, Carter C, Meier W (2010) Temporally resolved planar measurements of transient phenomena in a partially pre-mixed swirl flame in a gas turbine model combustor. *Combust Flame* 157(8):1510–1525

2. Caux-Brisebois V, Steinberg AM, Arndt CM, Meier W (2014) Thermo-acoustic velocity coupling in a swirl stabilized gas turbine model combustor. *Combust Flame* 161(12):3166–3180
3. Colin O, Ducros F, Veynante D, Poinso T (2000) A thickened flame model for large eddy simulations of turbulent premixed combustion. *Phys Fluids* (1994-present) 12(7):1843–1863
4. Dubief Y, Delcayre F (2000) On coherent-vortex identification in turbulence. *J Turbul* (1)
5. Franzelli B, Riber E, Sanjose M, Poinso T (2010) A two-step chemical scheme for kerosene-air premixed flames. *Combust Flame* 157(7):1364–1373
6. Galley D, Ducruix S, Lacas F, Veynante D (2011) Mixing and stabilization study of a partially premixed swirling flame using laser induced fluorescence. *Combust Flame* 158(1):155–171
7. Guedot L, Lartigue G, Moureau V (2015) Design of implicit high-order filters on unstructured grids for the identification of large-scale features in large-eddy simulation and application to a swirl burner. *Phys Fluids* (1994-present) 27(4):045107
8. Hannebique G (2013) Etude de la structure des flammes diphasiques dans les brûleurs aéronautiques. PhD thesis
9. Hunt JCR, Wray AA, Moin P (1988) Eddies, streams, and convergence zones in turbulent flows, pp 193–208
10. Jones W, Lettieri C, Marquis AJ, Navarro-Martinez S (2012) Large eddy simulation of the two-phase flow in an experimental swirl-stabilized burner. *Int J Heat Fluid Flow* 38:145–158
11. Lecourt R, Linassier G, Lavergne G (2011) Detailed characterisation of a swirled air/kerosene spray in reactive and non-reactive conditions downstream from an actual turbojet injection system. In: ASME 2011 turbo expo: turbine technical conference and exposition. American Society of Mechanical Engineers, pp 185–194
12. Légier J, Poinso T, Veynante D (2000) Dynamically thickened flame model for premixed and non-premixed turbulent combustion. In: Proceedings of the summer program. Citeseer, pp 157–168
13. Lucca-Negro O, O'doherty T (2001) Vortex breakdown: a review. *Prog Energy Combust Sci* 27(4):431–481
14. Moureau V, Bérat C, Pitsch H (2007) An efficient semi-implicit compressible solver for large-eddy simulations. *J Comput Phys* 226(2):1256–1270
15. Moureau V, Domingo P, Vervisch L (2011) Design of a massively parallel cfd code for complex geometries. *Comptes Rendus Mécanique* 339(2–3):141–148. <http://dx.doi.org/10.1016/j.crme.2010.12.001>
16. Nabil T, Kareem WA, Izawa S, Fukunishi Y (2000) Extraction of coherent vortices from homogeneous turbulence using curvelets and total variation filtering methods. *J Turbul* 57:76–86
17. Poinso T, Veynante D (2011) Theoretical and numerical combustion
18. Providakis T, Zimmer L, Scouffaire P, Ducruix S (2013) Characterization of the coherent structures in swirling flames stabilized in a two-staged multi-injection burner: Influence of the staging factor. *C R Mécanique* 341(1):4–14
19. Roux S, Lartigue G, Poinso T, Meier U, Bérat C (2005) Studies of mean and unsteady flow in a swirled combustor using experiments, acoustic analysis, and large eddy simulations. *Combust Flame* 141(1–2):40–54
20. Sanjosé M, Senoner J, Jaegle F, Cuenot B, Moreau S, Poinso T (2011) Fuel injection model for euler-euler and euler-lagrange large-eddy simulations of an evaporating spray inside an aeronautical combustor. *Int J Multiph Flow* 37(5):514–529
21. Steinberg AM, Boxx I, Stöhr M, Meier W, Carter CD (2012) Effects of flow structure dynamics on thermoacoustic instabilities in swirl-stabilized combustion. *AIAA J* 50(4):952–967
22. Stöhr M, Boxx I, Carter C, Meier W (2011) Dynamics of lean blowout of a swirl-stabilized flame in a gas turbine model combustor. *Proc Combust Inst* 33(2):2953–2960
23. Syred N (2006) A review of oscillation mechanisms and the role of the precessing vortex core (PVC) in swirl combustion systems. *Prog Energy Combust Sci* 32(2):93–161



<http://www.springer.com/978-3-319-60386-5>

Turbulence and Interactions

Proceedings of the TI 2015 Conference, June 11-14,
2015, Cargèse, Corsica, France

Deville, M.O.; Couaillier, V.; Estivalezes, J.-L.; Gleize, V.;
Lê, T.H.; Terracol, M.; Vincent, S. (Eds.)

2018, XVI, 280 p. 157 illus., 125 illus. in color.,

Hardcover

ISBN: 978-3-319-60386-5